Quantifying the Sensitivity of Precipitation to the Long-Term Warming Trend and Interannual–Decadal Variation of Surface Air Temperature over China

CHUNLÜE ZHOU AND KAICUN WANG

College of Global Change and Earth System Science, Beijing Normal University, Beijing, China

(Manuscript received 13 July 2016, in final form 18 January 2017)

ABSTRACT

Precipitation is expected to increase under global warming. However, large discrepancies in precipitation sensitivities to global warming among observations and models have been reported, partly owing to the large natural variability of precipitation, which accounts for over 90% of its total variance in China. Here, the authors first elucidated precipitation sensitivities to the long-term warming trend and interannual–decadal variations of surface air temperature T_a over China based on daily data from approximately 2000 stations from 1961 to 2014. The results show that the number of dry, trace, and light precipitation days has stronger sensitivities to the warming trend than to the T_a interannual–decadal variation, with 14.1%, −35.7%, and −14.6% K^{-1} versus 2.7%, −7.9%, and −3.1% K^{-1}, respectively. Total precipitation frequency has significant sensitivities to the warming trend (−18.5% K^{-1}) and the T_a interannual–decadal variation (−3.6% K^{-1}) over China. However, very heavy precipitation frequencies exhibit larger sensitivities to the T_a interannual–decadal variation than to the long-term trend over Northwest and Northeast China and the Tibetan Plateau. A warming trend boosts precipitation intensity, especially for light precipitation (9.8% K^{-1}). Total precipitation intensity increases significantly by 13.1% K^{-1} in response to the warming trend and by 3.3% K^{-1} in response to the T_a interannual–decadal variation. Very heavy precipitation intensity also shows significant sensitivity to the interannual–decadal variation of T_a (3.7% K^{-1}), particularly in the cold season (8.0% K^{-1}). Combining precipitation frequency and intensity, total precipitation amount has a negligible sensitivity to the warming trend, and the consequent trend in China is limited. Moderate and heavy precipitation amounts are dominated by their frequencies.

1. Introduction

Precipitation has undergone notable changes with respect to its frequency, intensity, duration, and amount over the past several decades (IPCC 2013). Many of these changes have important effects on human societies and natural ecosystems (Field et al. 2014). For instance, increases in intense precipitation have led to more flood disasters and soil erosion (Martínez-Casasnovas et al. 2002; Siswanto et al. 2015), while decreases in trace and light precipitation have led to risks of agriculture drought (Mishra and Liu 2014).

Human-induced warming is expected to induce changes in precipitation, but the magnitude of precipitation response or sensitivity to the warming and the underlying mechanisms are still being debated (Trenberth et al. 2003; Zhang et al. 2007; Min et al. 2011; Chou et al. 2012; Marvel and Bonfils 2013). Theoretically, a change in precipitation amount is argued to be associated with a change in atmosphere water vapor content, which increases with rising air temperature T_a by approximately 7% K^{-1} based on the Clausius–Clapeyron equation under a constant relative humidity (Trenberth 1998; Allen and Ingram 2002; Trenberth et al. 2003).

Further studies have revealed that additional latent heating from increased moisture convergence could further intensify rainstorms, which could lead to a larger than 7% K^{-1} increase for intense precipitation (Trenberth et al. 2003) and then further stabilize the atmosphere (O'Gorman and Schneider 2009a). As a consequence,

Denotes content that is immediately available upon publication as open access.

Supplemental information related to this paper is available at the Journals Online website: http://dx.doi.org/10.1175/JCLI-D-16-0515.s1.

Corresponding author e-mail: Kaicun Wang, kcwang@bnu.edu.cn

DOI: 10.1175/JCLI-D-16-0515.1

heavy precipitation events may become more common under global warming. In contrast, decreases in light to moderate precipitation may have been seen in observations over most land areas (Karl and Knight 1998; Liu et al. 2009; Shiu et al. 2012; Wasko and Sharma 2015) and in climate models (Kharin et al. 2007; Sun et al. 2007; Allan and Soden 2008; Lenderink and Van Meijgaard 2008).

Global-mean precipitation is projected to increase only by approximately 1%–3% K^{-1} global warming induced by anthropogenic forcing, and it is the same as for global evaporation rate, which is constrained by the global surface energy balance (Cubasch et al. 2001; Allen and Ingram 2002; Sun et al. 2007; Stephens and Ellis 2008).

However, interannual–decadal variations of linearly detrended precipitation frequency, intensity, and amount account for more than 66% ± 18% (mean ± standard deviation), 86% ± 11%, and 94% ± 5%, respectively, of their total variance in China for the period from 1961–2014 (Fig. S1 in the supplementary material), suggesting that interannual–decadal variation of precipitation plays a key role.

Numerous studies have linked interannual–decadal variation of precipitation to large-scale circulations using observational data and global models (Barnston and Livezey 1987; Wang and Zhou 2005; Chou and Tu 2008; Lu et al. 2008). These studies revealed generally distinct patterns and dynamical processes compared with those associated with the warming trend (Lenderink and Van Meijgaard 2008). Among these processes, upward vertical velocity may produce more precipitation extremes for interannual variations than for a warming trend (Allen and Ingram 2002; O'Gorman and Schneider 2009b).

Generally, ENSO dominates the interannual climate variability over the tropics, and its low-frequency variability further extends the effect to decadal–multidecadal time scales and to the mid-to-high latitudes (Trenberth et al. 1998; Dai and Wigley 2000; Dai 2001; Smith et al. 2006; Dai 2013; Dong and Dai 2015). Specifically, the positive phase of ENSO tends to be associated with more precipitation extremes in the tropics (Allan and Soden 2008; O'Gorman 2012) and in Australia over the last two millennia (Denniston et al. 2015). An ENSO-linked shift of storm tracks will change the precipitation pattern in midlatitudes (Trenberth et al. 2003); changes in large-scale atmospheric circulations, including the poleward propagation of westerlies and increase in surface pressure, partly result in precipitation decline over parts of southern Australia (Delworth and Zeng 2014).

Therefore, further research is required regarding the response of precipitation to interannual–decadal variation of T_a. In particular, the extent to which varying-intensity precipitation events are sensitive to interannual–decadal variation of T_a helps to advance the understanding of precipitation response.

Existing studies have attempted to investigate the relationship between interannual changes in precipitation and T_a. For example, Trenberth and Shea (2005) suggested a positive interannual correlation between precipitation and temperature over the tropical Pacific related to ENSO and in mid-to-high latitudes associated with the warm-moist advection in extratropical storms in winter. In addition, a negative correlation occurs over continental land in summer (Trenberth and Shea 2005). Wu et al. (2013) further pointed out that climate models involved in phase 5 of the Coupled Model Intercomparison Project (CMIP5) had difficulty in modeling the interannual correlation between precipitation and temperature in the warm season (May–September) in the midlatitudes of both hemispheres.

There is still a large discrepancy in the response of precipitation to change in T_a even using observational and reanalysis data, partly because most previous studies did not separate the response of precipitation to the long-term warming trends and that to the interannual–decadal variation in T_a. For example, Liu et al. (2009) and Shiu et al. (2012) reported an increase of heavy precipitation by approximately 100% K^{-1} and a decrease of light and moderate precipitation by approximately 20% K^{-1} based primarily on interannual differences of precipitation and T_a from 1979 to 2007. Liu and Allan (2012) revealed a negative sensitivity (from −8% to −11% K^{-1}) of satellite-derived precipitation to interannual change in T_a (not detrended) from 1998 to 2008 over tropical land (30°N–30°S). Westra et al. (2013) reported a significant increasing trend in annual maximum daily precipitation over the globe with the median sensitivities being 5.9% (from 1900 to 1959) and −7.7% K^{-1} (from 1960 to 2009) for the long-term changes. Ma et al. (2015) revealed a decrease of −17% K^{-1} in precipitation frequency with a maximum of −47% K^{-1} in dry days from 1960 to 2013 over China using the same interannual difference method used in Liu et al. (2009).

Studies have shown that precipitation exhibits a gamma distribution (Mooley 1973; Zhang et al. 2007; Westra et al. 2014) and has large spatiotemporal variation; thus, the mechanisms underlying the responses of precipitation may differ at various spatiotemporal scales. At seasonal time scales, some observations reveal an asymmetric response of seasonal precipitation (Allan and Soden 2008; Lenderink and Van Meijgaard 2010), thereby increasing the difference between wet and dry season precipitation (Chou et al. 2013).

Although changes in precipitation characteristics have been investigated, their association with the warming

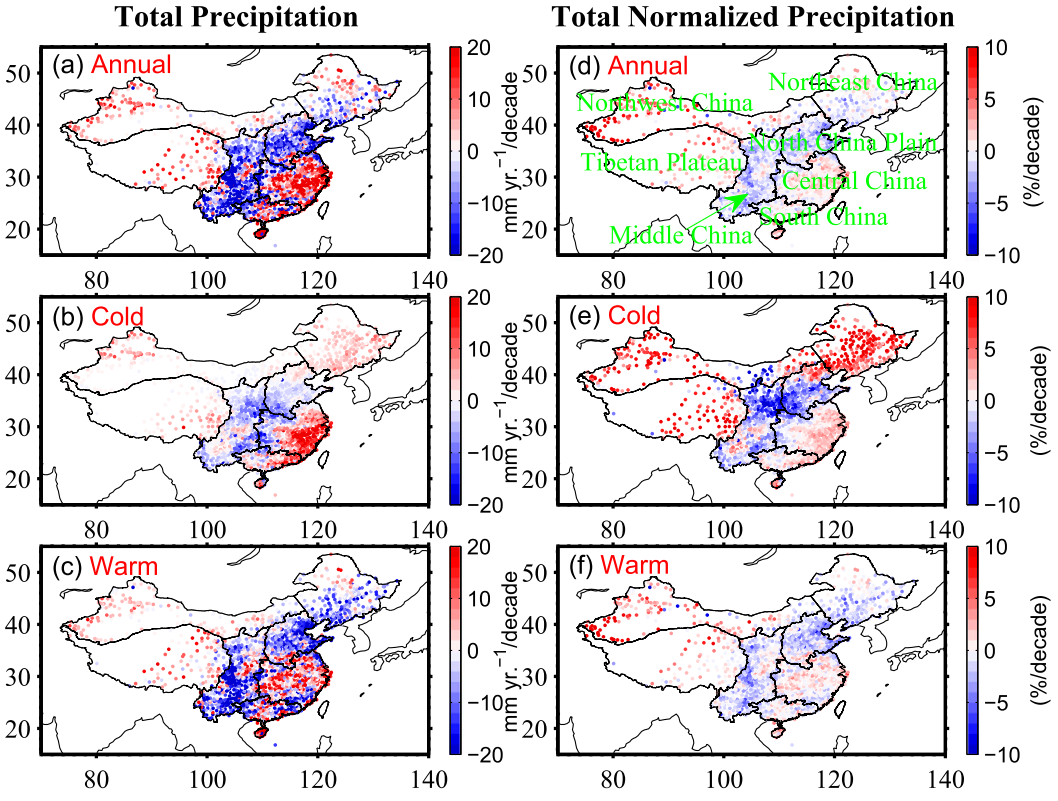

FIG. 1. Trend maps of (a) annual, (b) cold, and (c) warm seasonal total precipitation amounts (mm yr^{-1} $decade^{-1}$), and (d)–(f) as in (a)–(c), but their normalizations (% $decade^{-1}$) over China during the period 1961–2014. China is divided into seven subregions denoted in green in (b): Northwest China, the Tibetan Plateau, Middle China, Northeast China, the North China Plain, Central China, and South China.

trend remains unclear (O'Gorman and Schneider 2009b; Chou et al. 2012; Ma et al. 2015), especially at seasonal time scales. Moreover, the response of precipitation in terms of frequency, intensity, and amount to the interannual–decadal variation of T_a has seldom been investigated. In this study, we analyzed the latest comprehensive datasets to show how precipitation characteristics change with the long-term trend and interannual–decadal variation of T_a. This investigation helps advance our understanding of the impacts of climate change and variability on precipitation.

2. Data and methods

a. Precipitation and temperature data

The latest comprehensive dataset, including daily precipitation P and 2-m air temperature from approximately 2400 meteorological stations during the period 1961–2014 in China, was obtained from the China Meteorological Administration (CMA; http://data.cma.cn/en). This dataset has been subjected to quality control by the CMA. The quality control included the identification of outliers, an internal consistency check, spatial and temporal consistency checks, and artificial checks and correction of suspected and erroneous data.

To reduce impacts associated with data sampling and record length, the stations were preliminarily required to have no less than half of the record duration at all time scales: more than half of the entire study period (≥27 yr during the period 1961–2014), half of the reference period (≥15 yr during the period 1981–2010), half of the starting period (≥5 yr during the period 1961–70), half of the ending period (≥7 yr during the period 2001–14), and half of a month, season, and year for calculation of the corresponding values. As a result, approximately 2000 stations met the requirements and were used in this study (Fig. 1).

Among these about 2000 stations, approximately 95.6% (93.8%) of sites have more than 303 (365) days yr^{-1} and more than 50 yr of available precipitation data, and approximately 96.2% (93.4%) of sites have more than 304 (365) days yr^{-1} and more than 50 yr of available temperature data (Fig. S2 in the supplementary material), so the impact associated with data sampling and record length of precipitation and temperature datasets is limited and negligible. Moreover, data record lengths of precipitation and temperature datasets

have insignificant spatial patterns (Fig. S2). The stations are almost uniformly distributed across China, but their distribution is sparse on the western Tibetan Plateau (Fig. 1), despite the latest precipitation and temperature datasets used in this study.

b. Precipitation classification

In this study, a precipitation event is defined as one day with precipitation of no less than 0.1 mm daily or trace precipitation. A day with no precipitation (P = 0 mm daily) is considered a dry day. According to the CMA standards, a precipitation event is categorized into five intensity categories: trace ($0 < P < 0.1$ mm daily or flagged with "32700"), light ($0.1 \le P < 10$ mm daily), moderate ($10 \le P < 25$ mm daily), heavy ($25 \le P < 50$ mm daily), and very heavy ($P \ge 50$ mm daily). These classification criteria are used in many global analyses of precipitation (Dai 2006; Sun et al. 2007; Ma et al. 2015; Huang et al. 2016).

To depict the changes in precipitation characteristics, precipitation frequency, intensity, and amount were used. Precipitation frequency (in percent) was calculated as the ratio of the number of days with daily precipitation falling within each category to the number of days with available data during a certain period (i.e., a year or a season). Precipitation intensity was calculated as mean precipitation rates averaged among the precipitation events within a category. The precipitation amount in each category is the accumulated precipitation amount among the precipitation events within the category.

c. Calculation of long-term and interannual–decadal sensitivities of precipitation and their uncertainties

The trends in two time series inevitably affect the estimation of their cross correlation; this effect can be technically eliminated via detrended analysis (Podobnik and Stanley 2008). The detrended time series analysis has been widely used in climate studies: for example, paleoclimate temperature reconstructions (Conroy et al. 2009), coupling of atmospheric CO_2 and global climate (Veizer et al. 2000), and surface control (vegetation and soil) of diurnal temperature range in Sahel (Zhou et al. 2007). From technical and numerical analysis, the sensitivities of precipitation to the long-term warming trend and the interannual–decadal variation of T_a can be disentangled using detrended and regression analysis.

Specifically, precipitation characteristics P (including frequency, intensity, and amount) were summed from the precipitation trend term $P_{\rm tr}$ and the interannual–decadal variation term P_v [expressed in Eq. (1)]. The term T_a was summed from the temperature trend term $T_{\rm tr}$ and temperature variability term T_v [expressed in Eq. (2)]. A linear least squares analysis with the Student's t test of significance and an estimation of the standard deviation of trend was adopted for the trend in precipitation characteristics tr_P and surface air temperature tr_T with time t [Eqs. (1) and (2)].

Thus, the sensitivity of precipitation to a warming trend α is the ratio of the trend in precipitation tr_P to the trend in temperature tr_T [expressed as Eq. (3)].

$$P = \mathrm{tr}_P t + P_v = P_{\rm tr} + P_v, \tag{1}$$

$$T = \mathrm{tr}_T t + T_v = T_{\rm tr} + T_v, \quad \text{and} \tag{2}$$

$$\alpha = \frac{\Delta P_{\rm tr}}{\Delta T_{\rm tr}} = \frac{\Delta P_{\rm tr}/\Delta t}{\Delta T_{\rm tr}/\Delta t} = \frac{\mathrm{tr}_P}{\mathrm{tr}_T}. \tag{3}$$

A linear regression slope k of P_v against T_v with 95% confidence intervals, based on the Student's t test of significance [expressed in Eq. (4)], is used to calculate the sensitivity β of precipitation to interannual–decadal variation of T_a [expressed as Eq. (5)].

$$P_v = kT_v + \varepsilon \quad \text{and} \tag{4}$$

$$\beta = \frac{\Delta P_v}{\Delta T_v} = \frac{k\Delta T_v}{\Delta T_v} = k. \tag{5}$$

where ε is the regression residual via the least squares method, whose expected value is close to zero.

To estimate 95% confidence intervals of trend ratios, we used 2000 bootstrap statistical resamplings based on a normal distribution with mean and standard deviation parameters of tr_P and tr_T. Using the percentile bootstrap confidence interval method (Efron and Tibshirani 1994), an estimated 95% confidence interval can be acquired. To ensure the robustness of the confidence interval, we repeated the above processes 200 times and regarded their median as the final confidence interval (Krzywinski and Altman 2014). The more bootstrap samples are processed, the higher the accuracy of these percentiles will become (Kulesa et al. 2015).

To calculate nationally and regionally averaged precipitation sensitivities, we first computed each station's precipitation frequency, intensity, and amount in each category and gridded them onto $1^\circ \times 1^\circ$ longitude–latitude grids for the period 1961–2014 period; we further normalized them based on their corresponding multiyear averages, expressed as a percentage. Such gridded calculation was correspondingly conducted for T_a over China and its subregions. Note that the warm season is defined from May to October and the cold season is defined from November to April.

Here, we selected T_a as a dependent variable of precipitation response for two reasons: 1) to remain consistent with previous studies for convenient comparison (Sun et al. 2007; Liu et al. 2009; O'Gorman and

Schneider 2009b; Ma et al. 2015) and 2) because change in T_a is an integrated and known result of the warming trend, atmospheric circulations, atmospheric moisture, and local surface conditions and helps to quantify the sensitivities of precipitation to the warming trend and interannual–decadal variation of T_a. Since T_a and atmospheric moisture are closely correlated at a local scale, following Trenberth and Shea (2005), we selected national and regional mean T_a as reference temperatures, rather than global mean T_a.

3. Results

a. Changes in precipitation characteristics over China

To better understand the long-term change in precipitation, Fig. 1 displays the geographic distributions of trends in annual and seasonal precipitation totals during the period 1961–2014 together with their normalizations (by multiyear averages). Trends of precipitation amount have an evident pattern, with remarkable increases over dry regions of western China and the Tibetan Plateau and decreases in the North China Plain and Middle China (Figs. 1b,c,e,f).

The pattern of annual precipitation trends is overall similar to that based on previous versions of precipitation dataset with about 740 stations (Wang and Zhou 2005; Zhai et al. 2005) but exhibits more homogeneity with the neighborhoods and more details in eastern China (Fig. 1). Precipitation trends over China by the use of the latest version of precipitation are slightly larger than those by the use of the previous version of precipitation: that is, −0.93% versus −1.25% decade^{-1} ($p < 0.05$, from the latest version versus the previous version of precipitation) for light precipitation, −0.7% versus −1.14% decade^{-1} ($p < 0.05$) for moderate precipitation, 0.41% versus 0.22% decade^{-1} ($p > 0.05$) for heavy precipitation, and 2.23% versus 2.01% decade^{-1} ($p < 0.05$) for very heavy precipitation (Fig. 2c) revealed by Ma et al. (2015). This situation occurs for precipitation frequency, especially for very heavy precipitation frequency [1.87% ($p < 0.05$) vs 1.51% decade^{-1} ($p < 0.1$); Fig. 2a]. These results indicate that the latest version of precipitation with more complete coverage can better depict the changes in precipitation characteristics.

We further found that trends in precipitation totals are comparable in both seasons (Figs. 1b,c), although normalized changes in the cold season are notably greater than those in the warm season, especially in northern China and on the Tibetan Plateau (Figs. 1e,f). The precipitation amount over Middle China and Northeast China exhibits an opposite long-term change for both cold and warm seasons (Figs. 1b,c,e,f).

Over China, the increase in the frequency of dry days (normalized by their multiyear averages) was over 1.7-fold greater in the warm season (4.2% decade^{-1}; $p < 0.05$) than in the cold season (2.5% decade^{-1}; $p < 0.05$) (Figs. 2b,c). The increase in the number of dry days would suppress precipitation frequency, which decreased by a rate of approximately 4% decade^{-1} ($p < 0.05$; Figs. 2a–c). However, the constituent structures of decrease in precipitation frequency differ between the two seasons. In the cold season, the decrease in the number of trace and light precipitation days counteracts the increase in heavy and very heavy precipitation frequencies (Fig. 2b), but in the warm season, the decrease in the number of trace to heavy precipitation days together constitutes an important decrease in precipitation frequency (Fig. 2c). Moreover, increases in heavy and very heavy precipitation frequency are much faster in the cold season than in the warm season over China [2.5% vs −0.03% decade^{-1} ($p > 0.05$) and 4.9% vs 1.4% decade^{-1} ($p < 0.05$); Figs. 2b,c]. In addition, the number of trace days in China decrease by the highest rate (~8% decade^{-1}; $p < 0.05$) among all groups at annual and seasonal time scales (Figs. 2a–c). These results are roughly consistent with those based on previous version of precipitation dataset during study period of 1960–2013 (Ma et al. 2015).

Precipitation intensity in six categories uniformly strengthens at all time scales over China, except for Northeast China and the North China Plain (Figs. 2d–f). This mainly results from a combination of water vapor increase due to a warming trend and changes in large-scale circulations (Emori and Brown 2005; Trenberth and Shea 2005; Chou et al. 2012). It is worth noting that very heavy precipitation intensity strengthens in the cold season over China (Fig. 2e). An existing study reported a significant increase of total precipitation in the cold season from 1951 to 2000 over China (Zhai et al. 2005), and our study goes further to show that the increase is due to the substantial increase in very heavy precipitation.

The annual precipitation amount remains roughly constant over China (~0.08% decade^{-1}; $p > 0.05$; Fig. 2g), exhibiting a seasonality that increases by 1.04% decade^{-1} ($p < 0.05$) in the cold season and decreases by −0.28% decade^{-1} ($p > 0.05$) in the warm season (Figs. 2h,i), which would narrow the range of seasonal precipitation in China. Very heavy precipitation amount increases more in the cold season (4.78% decade^{-1}; $p < 0.05$) than in the warm season (1.84% decade^{-1}; $p < 0.05$) (Figs. 2h,i). Zhai et al. (2005) pointed out that the increase of precipitation in the cold season is stronger than that in the warm season. This study further points out that the increase is primarily due to the increase in very heavy precipitation. This provided independent evidence for an increase in precipitation

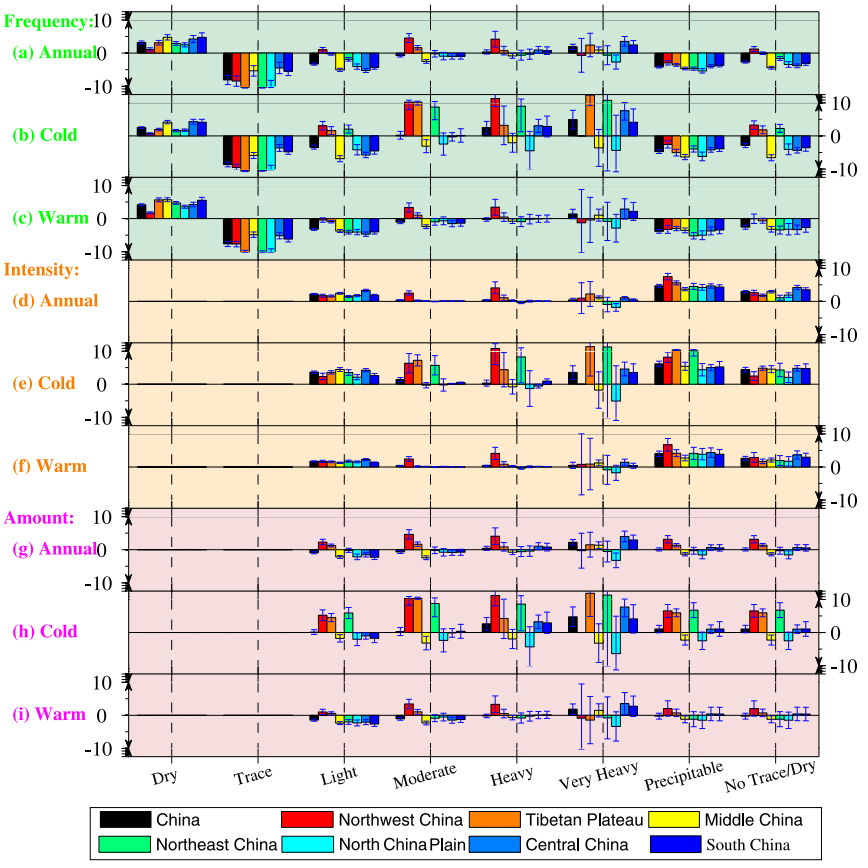

FIG. 2. Trends (% decade^{-1}) in (a)–(c) precipitation frequency, (d)–(f) intensity, and (g)–(i) amount for eight categories, including dry, trace, light, moderate, heavy, very heavy, precipitable, and no trace/dry days at annual, cold, and warm seasonal time scales over seven subregions of China (denoted in green in Fig. 1b) during the period 1961–2014. The precipitation characteristics are normalized by their multiyear averages during the study period. According to the CMA standards (http://data.cma.cn/en), the precipitation is categorized into five intensity bins: trace ($0 < P < 0.1$ mm daily), light ($0.1 \le P < 10$ mm daily), moderate ($10 \le P < 25$ mm daily), heavy ($25 \le P < 50$ mm daily), and very heavy ($P \ge 50$ mm daily). A dry day is a day without precipitation, a precipitable day is a day with more than 0 precipitation, and a no trace/dry day is a day with measurable precipitation (i.e., ≥0.1 mm daily). The blue error bars overlaid on the colored bars denote a 95% confidence interval based on the two-tailed Student's t test. Because of the rare occurrence of very heavy precipitation in the cold season over Northwest China, the trends in very heavy precipitation characteristics are not estimated here.

extremes over dryland under global warming (Guillod et al. 2015; Donat et al. 2016).

b. *Changes in precipitation characteristics over China's subregions*

To elaborate changes in precipitation characteristics in terms of frequency, intensity, and amount, mainland China was divided into seven subregions: namely, Northwest China, the Tibetan Plateau, Middle China, Northeast China, the North China Plain, Central China, and South China. Similar subregions have been widely adopted in research on precipitation over China (Liu et al. 2005; Zhai et al. 2005; Jiang et al. 2014; Ma et al. 2015).

Changes in the number of dry and trace days over seven subregions are similar to those over China, and hence precipitation frequency over all of the subregions shows a consistent decrease with that over China (Figs. 2a–c). However, light–very heavy precipitation frequencies over subregions exhibit incoherent patterns with those over China (Figs. 2a–c). In particular, light and moderate precipitation frequencies significantly increase over Northwest China, the Tibetan Plateau, and Northeast China in the cold season but decrease over the

other subregions (Fig. 2b). Heavy precipitation frequencies significantly increase in the cold season over Northwest China, Northeast China, Central China, and South China (Fig. 2b). Very heavy precipitation frequencies significantly increase in the cold season over the Tibetan Plateau, Central China, and South China (Fig. 2b). Overall, changes in moderate–very heavy precipitation frequencies in the cold season are larger than those in the warm season over the seven subregions (Figs. 2b,c).

Precipitation intensity in most categories significantly strengthens over the seven subregions, similar to that over China, especially uniform for light and total precipitation intensity (Figs. 2d–f). Yet moderate to very heavy precipitation intensities have evidently spatial variance. Strength in moderate and heavy precipitation intensity over Northwest China (Figs. 2d–f) is closely related to temperature rise and potential vorticity anomalies (Zhou and Huang 2010).

Very heavy precipitation intensity over the North China Plain decreases likely as a result of the weakening of the East Asian summer monsoon since the 1970s (Wang 2001), which would meanwhile cause more precipitation in southern China (Figs. 2d–f). Significant weakening of the East Asian winter monsoon since the 1980s (Wang et al. 2009b) promotes very heavy precipitation intensity over Northeast China in the cold season (Fig. 2e), whose water vapor originates from the northwestern Pacific (Wang et al. 2009a). Overall, precipitation intensity experiences more evident strength in the cold season ($\sim$6% decade^{-1}; $p < 0.05$) than in the warm season ($\sim$4% decade^{-1}; $p < 0.05$) (Figs. 2e,f).

The precipitation amount in all groups over Northwest China roughly increases at all time scales, especially larger in the cold season (Figs. 2g–i). Meanwhile in the cold season, light to very heavy precipitation amounts significantly increase over the Tibetan Plateau and Northeast China (Fig. 2h). In the warm season, light and moderate precipitation amounts primarily decrease over the seven subregions (Fig. 2i). Very heavy precipitation amount significantly increases over the Central China and South China at annual and seasonal time scales (Figs. 2g–i).

In addition to the weakening of the East Asian summer and winter monsoon (Wang 2001; Wang et al. 2009b), the increase in aerosol concentration possibly accounts for the decrease in precipitation amount in the North China Plain (Figs. 2g–i). The enhanced atmospheric stability by aerosol tends to depress upward vertical velocity and thereby restrain precipitation. Less precipitation will accelerate the accumulation of aerosol particles without a washout process and form a positive feedback (Xu 2001; Menon et al. 2002; Zhao et al. 2006).

c. *Sensitivities of precipitation to the long-term trend and interannual–decadal variation of air temperature over China*

Figure 3 shows the sensitivity of precipitation characteristics (including frequency, intensity, and amount) in eight categories for a warming trend and interannual–decadal variation of T_a. The frequencies of dry, trace, and light precipitation days in China are more sensitive to the warming trend [$\sim$14.1%, $-$35.7%, and $-$14.6% K^{-1} ($p < 0.05$) at annual time scales, respectively] than to interannual–decadal variation of T_a [$\sim$2.7%, $-$7.9%, and $-$3.1% K^{-1} ($p < 0.05$) at annual time scales, respectively] (Fig. 3). Previous studies did not disentangle the sensitivities of precipitation to the long-term trend and interannual–decadal variation of T_a (Lenderink and Van Meijgaard 2008; Liu et al. 2009; Shiu et al. 2012; Chou et al. 2013; Ma et al. 2015). For example, both mixed sensitivities of dry, trace, and light precipitation frequencies to change in T_a are 20.63%, $-$46.53%, and $-$22.38% K^{-1} ($p < 0.05$) over China, respectively (Ma et al. 2015), close to the sum of the sensitivities of their precipitation frequencies to the long-term trend and interannual–decadal variation of T_a in this study.

Negative sensitivities of trace and light precipitation frequencies in China explain most of the sensitivity of total precipitation frequency to a warming trend [$-$18.5%, $-$17.08%, and $-$21.70% K^{-1} ($p < 0.05$) at annual, cold, and warm seasonal time scales, respectively] and to the interannual–decadal variation of T_a [$-$3.6%, $-$3.22%, and $-$3.88% K^{-1} ($p < 0.05$) at annual, cold, and warm seasonal time scales, respectively] (Fig. 3). These findings imply that a warming trend plays a more important role in changes of dry, trace, and light precipitation frequencies than natural interannual variability does. This finding is applicable for subregions of China (Figs. 4–10).

Very heavy precipitation frequency in China is comparably sensitive to the warming trend (8.2% K^{-1}; $p < 0.05$) and interannual–decadal variation of T_a (6.1% K^{-1}; $p < 0.05$) at annual time scales (Figs. 3a,d), suggesting a similar role of warming trend and natural interannual variability. However, it varies by season; that is, the role of the warming trend of T_a (17.64% K^{-1}; $p < 0.05$) is stronger than that of natural interannual variability in the cold season (Figs. 3b,e), whereas it is the opposite in the warm season (7.78% vs 9.62% K^{-1}; $p < 0.05$; Figs. 3c,f), mainly because of the additional impact of convective process in the warm season (Emori and Brown 2005).

Moderate, heavy, and very heavy precipitation intensities in China are comparably sensitive to the warming trend

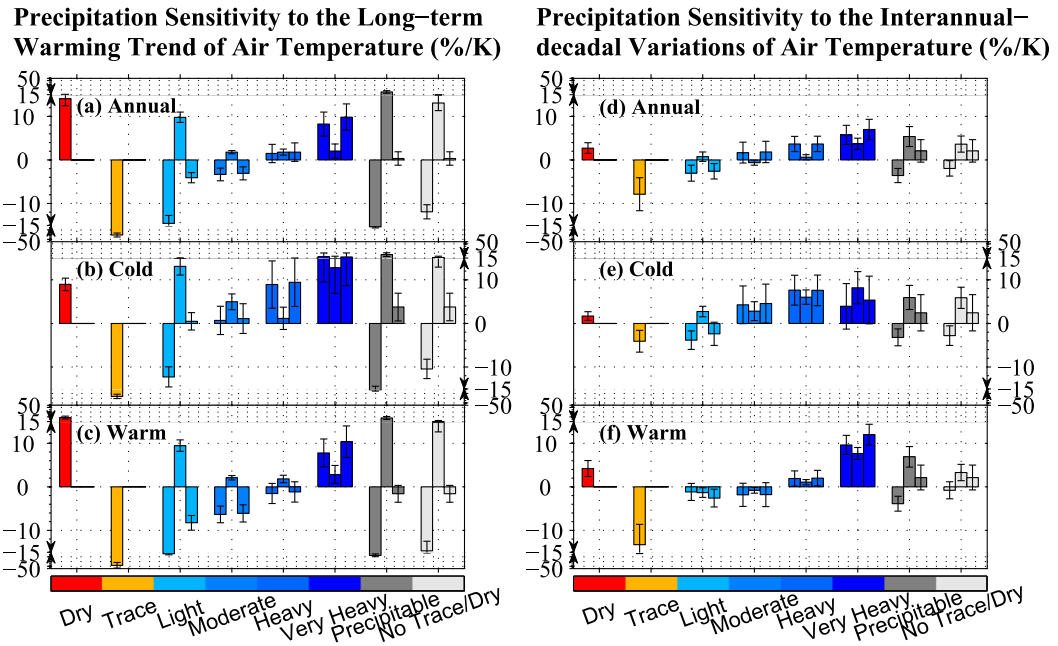

FIG. 3. Sensitivity (% K^{-1}) of precipitation frequency, intensity, and amount in eight precipitation categories, including dry, trace, light, moderate, heavy, very heavy, precipitable, and no trace/dry days, at annual, cold, and warm seasonal time scales over China is shown for (a)–(c) the long-term trend and (d)–(f) interannual–decadal variation of T_a. Each group of bars consists of sensitivities of precipitation frequency, intensity, and amount. The error bars overlaid on the colored bars denote a 95% confidence interval. According to the CMA standards (http://data.cma.cn/en), the precipitation is categorized into five intensity bins: trace ($0 < P < 0.1$ mm daily), light ($0.1 \le P < 10$ mm daily), moderate ($10 \le P < 25$ mm daily), heavy ($25 \le P < 50$ mm daily), and very heavy ($P \ge 50$ mm daily). A dry day is a day without precipitation, a precipitable day is a day with more than 0 precipitation, and a no trace/dry day is a day with measurable precipitation (i.e., ≥0.1 mm daily).

[1.8%, 1.8%, and 2.1% K^{-1} ($p < 0.05$) at annual time scales, respectively] and to the interannual–decadal variation of T_a [−0.7%, 0.6%, and 3.7% K^{-1} ($p < 0.05$) at annual time scales, respectively] (Fig. 3). Furthermore, the warming trend produces positive sensitivities of various precipitation intensities (Figs. 3a–c), which implies that the warming trend strengthens precipitation intensity, with annual sensitivity of 13.1% K^{-1} over China (Fig. 3a). Moderate, heavy, and very heavy precipitation amounts in China show similar sensitivities to the warming trend [−3.1% ($p < 0.05$), 1.8% ($p > 0.05$), and 9.8% K^{-1} ($p < 0.05$) at annual time scales, respectively] and to the interannual–decadal variation of T_a [1.8% ($p > 0.05$), 3.7% ($p < 0.05$), and 7.5% K^{-1} ($p < 0.05$) at annual time scales, respectively] (Fig. 3).

Accompanied by a decrease in light precipitation frequency, the warming trend enhances the water vapor holding capacity in the atmosphere and subsequently strengthens light precipitation intensity, with annual sensitivity of 9.8% K^{-1} ($p < 0.05$), if light precipitation occurs (Figs. 3a–c). Surprisingly, oppositely seasonal sensitivities of moderate precipitation occur for interannual–decadal variation of T_a (Figs. 3e,f), and the reasons are still unknown.

In all, the warming trend and interannual–decadal variation of T_a have more evident impacts on trace, light, and very heavy precipitation than on moderate and heavy precipitation. Moreover, the sensitivities of dry–heavy-grouped precipitation to the warming trend are often greater than those to the interannual–decadal variation of T_a. The warming trend strengthens precipitation intensity but reduces the precipitation frequency over China. Combining precipitation frequency and intensity, the sensitivities of light and moderate precipitation amounts to the warming trend and interannual–decadal variation of T_a are dominated by their frequencies, whereas the very heavy precipitation amount is both regulated by precipitation frequency and intensity (Fig. 3).

d. Sensitivities of precipitation to the long-term trend and interannual–decadal variation of air temperature over China's subregions

The sensitivities of moderate–very heavy precipitation frequencies to the long-term trend and interannual–decadal variation of T_a vary by subregions of China that owns vast territory and complex topography (Figs. 4–10). Over Northwest China, moderate and

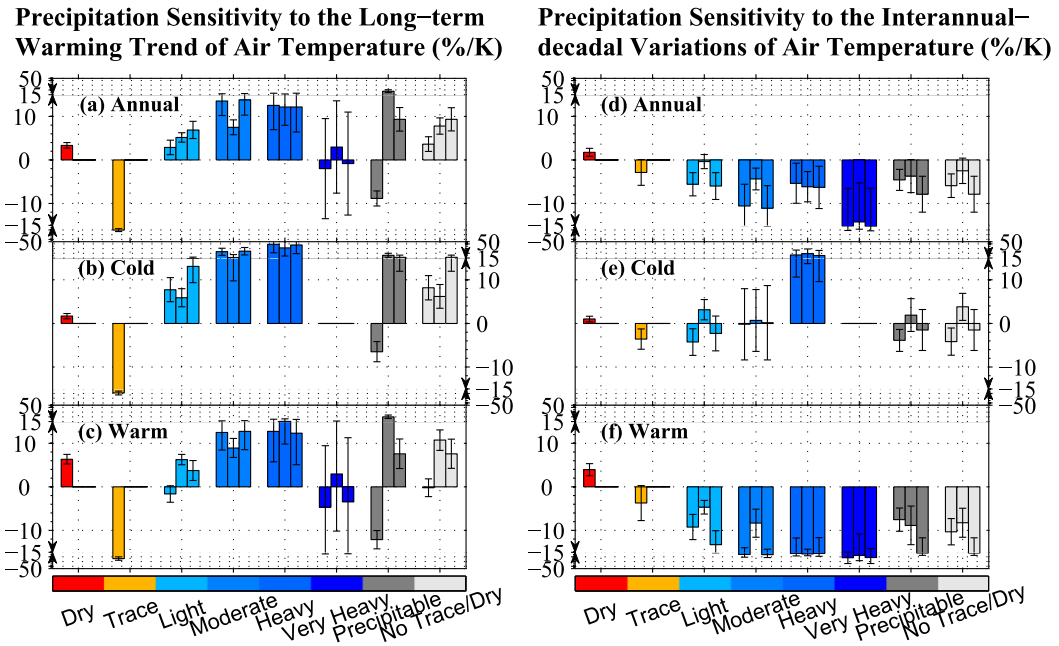

FIG. 4. As in Fig. 3, but for Northwest China. The sensitivities of very heavy precipitation characteristics to the long-term warming trend and interannual–decadal variation of T_a are not estimated during the cold season, because of the rare occurrence of very heavy precipitation in the cold season over Northwest China.

heavy precipitation frequencies consistently exhibit positive sensitivities to the long-term trend of T_a at annual, cold, and warm seasonal time scales (Figs. 4a–c), suggesting that moderate and heavy precipitation occurs more frequently under global warming. However, moderate–very heavy precipitation frequencies exhibit negative sensitivities to the interannual–decadal variation of T_a at annual and warm seasonal time scales (Figs. 4d,f).

Over Tibetan Plateau, moderate and very heavy precipitation frequencies are more sensitive to the long-term warming trend of T_a in the cold season (Figs. 5b,e), whereas heavy and very heavy precipitation frequencies

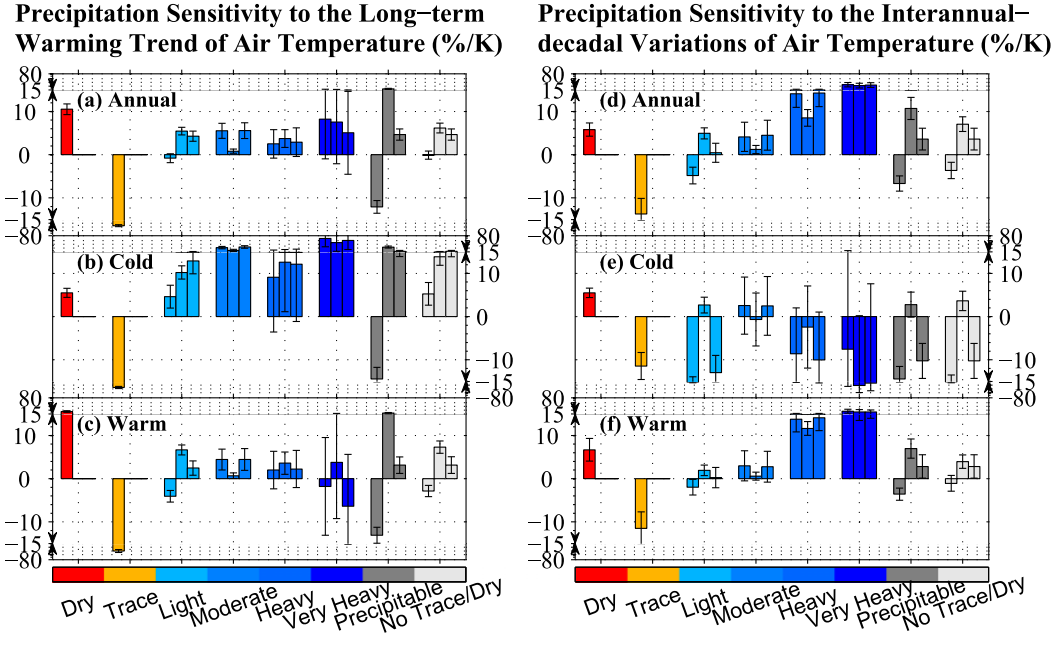

FIG. 5. As in Fig. 3, but for the Tibetan Plateau.

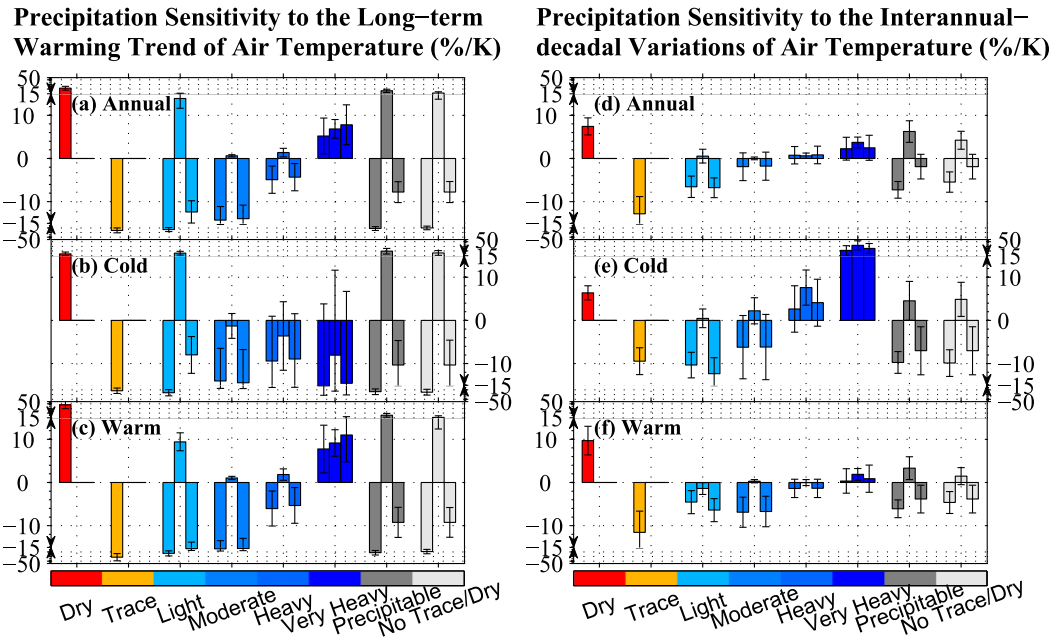

FIG. 6. As in Fig. 3, but for Middle China.

are more sensitive to the interannual–decadal variation of T_a in the warm season (Figs. 5c,f). The sensitivities of precipitation intensity and amount are roughly similar to those of precipitation frequency over Northwest China and the Tibetan Plateau (Figs. 4 and 5).

Over Middle China, moderate precipitation frequency decreases by −2.52%, −3.10%, and −2.42% decade^{-1} ($p < 0.05$) at annual, cold, and warm seasonal time scales, respectively (Figs. 1a–c), jointly resulting from negative responses to the long-term trend [−14.27%, −14.03%, and −18.17% K^{-1} ($p < 0.05$), respectively] and interannual–decadal variation of T_a [−1.91% ($p > 0.05$), −6.21% ($p > 0.05$), and −6.88% K^{-1} ($p < 0.05$), respectively] (Fig. 6). The responses of precipitation amounts show similarity to those of precipitation frequencies over Middle China (Fig. 6). Nevertheless, the sensitivities

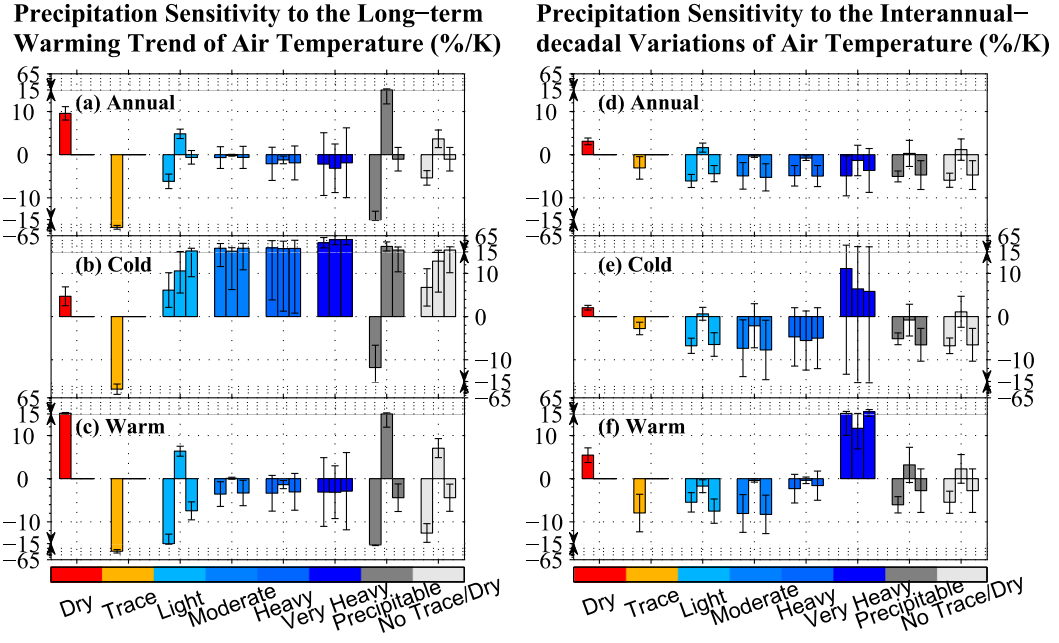

FIG. 7. As in Fig. 3, but for Northeast China.

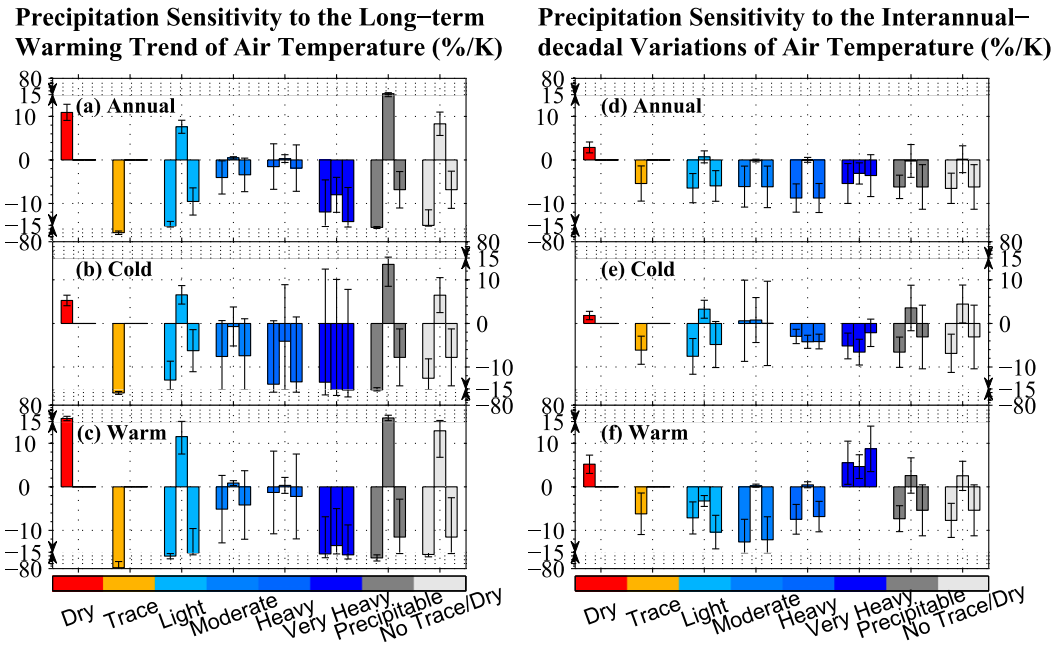

FIG. 8. As in Fig. 3, but for the North China Plain.

of precipitation intensity to the long-term trend [20.96%, 24.48%, and 20.15% K^{-1} ($p < 0.05$) at annual, cold, and warm seasonal time scale, respectively] is significantly larger than those to the interannual–decadal variation of T_a [6.23%, 4.53%, and 3.32% K^{-1} ($p < 0.05$) at annual, cold, and warm seasonal time scale, respectively] over Middle China (Fig. 6).

Over Northeast China, moderate–very heavy precipitation frequencies show positive sensitivities to the long-term trend of T_a in the cold season (25.95%, 26.83%, and 43.03% K^{-1}; $p < 0.05$; Fig. 7b), leading to their upward trends in the cold season [8.69% ($p < 0.05$), 9.00% ($p < 0.05$), and 1.44% K^{-1} ($p > 0.05$); Fig. 1b]. Very heavy precipitation exhibits a strong positive response to the interannual–decadal variation

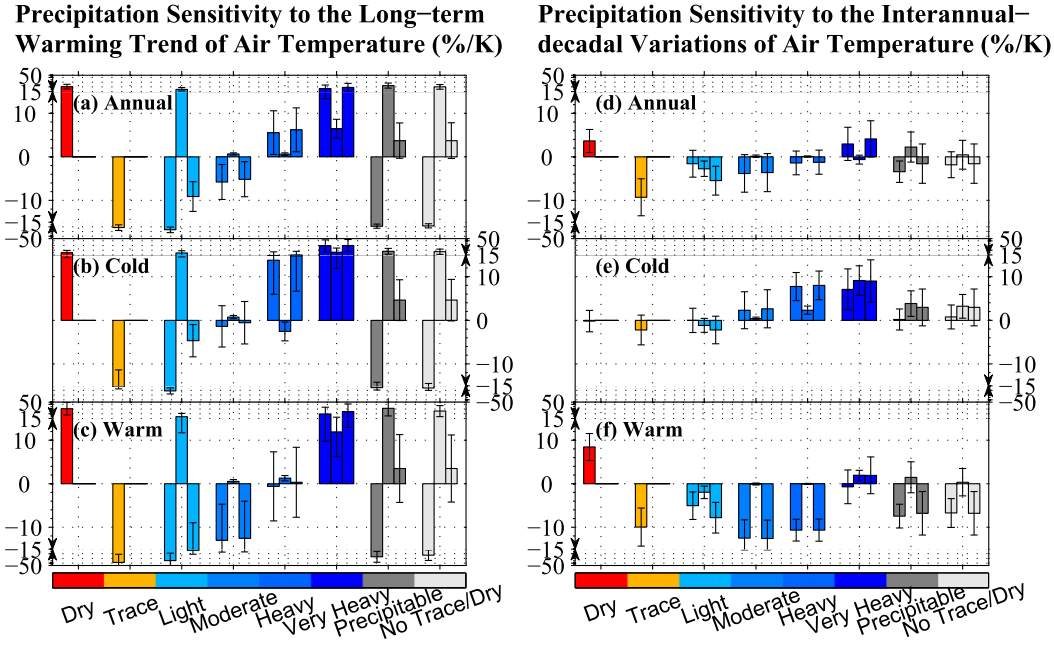

FIG. 9. As in Fig. 3, but for Central China.

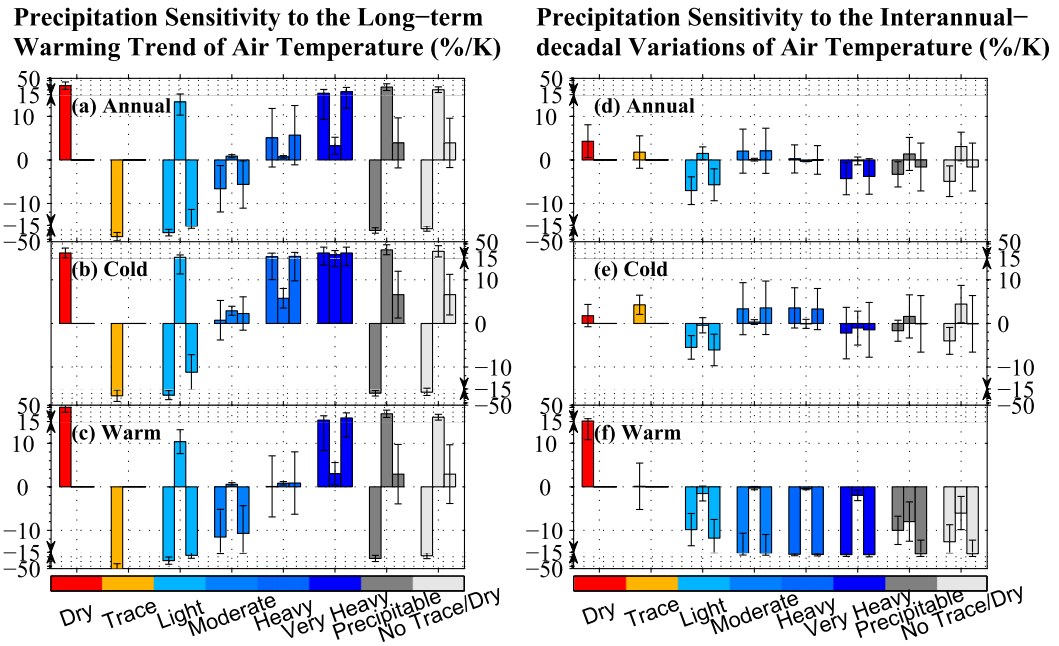

FIG. 10. As in Fig. 3, but for South China.

of T_a in the warm season, with 16.31%, 11.65%, and 21.28% K^{-1} for precipitation frequency, intensity, and amount, respectively (Fig. 7f).

Over the North China Plain, moderate and heavy precipitation present negative sensitivities to interannual–decadal variation of T_a in the warm season (−12.64% and −7.45% K^{-1}; $p < 0.05$ for precipitation frequency; −12.13% and −6.81% K^{-1}; $p < 0.05$ for precipitation amount), but very heavy precipitation shows a positive sensitivity (5.54%, 4.65%, and 8.72% K^{-1}; $p < 0.05$ for precipitation frequency, intensity, and amount, respectively) (Fig. 8f). Light precipitation frequency and amount present negative sensitivities to the long-term T_a at annual and seasonal time scales (Figs. 8a–c). These may be because the elevated anthropogenic aerosols in recent decades can suppress the onset of precipitation events, accumulate more atmospheric moisture, release more latent heat, invigorate stronger convection process, and then form more frequent precipitation extremes (Xu 2001; Zhao et al. 2006; Qian et al. 2009; Liu et al. 2015; Wang et al. 2016).

Over Central China and South China, heavy and very heavy precipitation frequencies are both positively sensitive to the long-term trend and interannual–decadal variation of T_a in the cold season (Figs. 9b,e and 10b,e), mainly because of the abundant moisture source from the western Pacific Ocean. The sensitivities of precipitation amount are dominated by those of precipitation frequency over Central China and South China (Figs. 9 and 10). The moderate and heavy precipitation frequency and amount exhibit opposite seasonal sensitivities to the interannual–decadal variation of T_a (Fig. 9 and 10). In addition, light precipitation frequency and amount exhibit negative sensitivities to the long-term T_a over Central China and South China (Figs. 9a–c), likely as a result of the effect of increasing anthropogenic aerosol (Fu and Dan 2014; Wang et al. 2016) through reducing cloud droplet size and then delaying raindrop formation (Cheng et al. 2005; Qian et al. 2009). This process could also result in positive long-term sensitivities of very heavy precipitation (Figs. 9a–c).

Taken together, the findings regarding precipitation frequency, intensity, and amount in each category over China and its subregions are roughly coordinated with each other, implying that the partitioning of sensitivities for the warming trend and interannual–decadal variation of T_a is robust over China and its subregions.

e. *Relationship between long-term and interannual–decadal sensitivities of precipitation over China*

Here, we showed that the nationally averaged sensitivities of precipitation (including frequency, intensity, and amount) to the interannual–decadal variations are strongly correlated with those to the long-term trend of T_a, with correlation coefficients of 0.84 ($p = 0.00$), although their magnitudes are not completely consistent (Fig. 11). Therefore, the sensitivities of precipitation to the interannual–decadal variation of T_a can be predicted by those to the warming trend with a prediction error of 2.86% K^{-1} (Fig. 11). It is worth noting that very heavy

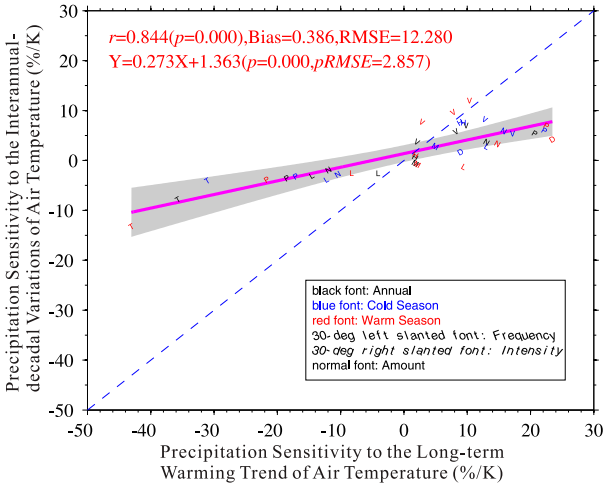

FIG. 11. Relationship between precipitation sensitivities (of precipitation frequency, intensity, and amount) to the warming trend and interannual–decadal variation of T_a with a significance level of 0.05 in China. The initial capitalized letters are used to represent the precipitation sensitivities among eight precipitation categories: dry days (D); trace days (T); light (L), moderate (M), heavy (H), and very heavy (V) precipitation; precipitable days (P); and no trace/dry days (N). The black, blue, and red characters denote annual, cold, and warm seasons, respectively. The 30° left (right)-slanted font denotes precipitation frequency (intensity), and the normal font denotes precipitation amount. Some statistics for both sensitivities, including correlation coefficient r with significance level p, bias, and RMSE, are listed. The predictable regression of sensitivity to the T_a interannual–decadal variation against that to the warming trend is also listed with regression slope, regression significance level p, and the predicted RMSE (pRMSE).

precipitation shows a similar sensitivity between to the interannual–decadal variation and to the long-term trend of T_a over China (along the 1:1 line in Fig. 11).

These results suggest that the processes governing the long-term sensitivities of precipitation should work to a certain extent in a similar way for the interannual–decadal sensitivities of precipitation, although in different magnitudes. In climate models, there is a general way to constrain the long-term feedbacks using short-term feedbacks (including from daily to interannual time scales; Knutti et al. 2006; O'Gorman 2012; Dalton and Shell 2013; Deangelis et al. 2015) because the short-term feedbacks could be conveniently validated with the limited observational data. O'Gorman (2012) reported a correlation coefficient of 0.866 between long-term and interannual–decadal sensitivities of the 99.99th precipitation percentile over global tropics across the CMIP3 models. Dai (2016) recently revealed similar relationships between interannual variation and long-term changes in air temperature and precipitable water from observation, CMIP3 and CMIP5 models and suggested many physical processes may work similarly in producing the interannual climate variations and the greenhouse gas (GHG)-induced long-term changes.

However, because of large natural variability in regional precipitation and temperature (Deser et al. 2012), our estimated long-term trends may still contain substantial contributions from internal climate variability that are not related to GHGs and other external forcing. Because of this, the precipitation sensitivity to the long-term warming trend estimated here may not be fully comparable with model-simulated precipitation response to global warming caused by GHGs and other external forcing.

f. Relationship between long-term and interannual–decadal sensitivities of precipitation over China's subregions

We further looked at the relationship between sensitivities of precipitation to the long-term trend and interannual–decadal variation of T_a in the seven subregions of China (Fig. 12). The slopes of the sensitivities of precipitation to the interannual–decadal variation of T_a against those to the long-term trend are significant: 0.23 ($p < 0.05$), 0.24 ($p < 0.05$), 0.27 ($p < 0.05$), 0.24 ($p < 0.05$), and 0.11 ($p < 0.05$) over Northwest China, the Tibetan Plateau, Middle China, Central China, and North China, respectively (Fig. 12). These slopes are very close to that over the whole of China, indicating that the relationship between the long-term and interannual–decadal sensitivities of precipitation is robust and region independent. The relatively small slope of 0.11 ($p < 0.05$) over the North China Plain (Fig. 12e) partly results from the different long- and short-term effects of aerosols (Liu et al. 2015).

The slopes are nonsignificant over another two regions, Northeast China (0.05; $p > 0.05$) and South China (0.10; $p > 0.05$) (Fig. 12). Further model research continues to lead to understanding these nonsignificant relationships. In addition, the correlation coefficients between the long-term and interannual–decadal sensitivities of precipitation over most regions [0.34, 0.48, 0.82, and 0.41 ($p < 0.05$) for Northwest China, the Tibetan Plateau, Central China, and the North China Plain, respectively] are smaller than that over the whole of China (0.84; $p < 0.05$) (Figs. 11 and 12). This indicates that the long-term and interannual–decadal sensitivities of precipitation to T_a over subregions contain many regional details and thereby the relationship of both sensitivities is more robust over the whole of China.

4. Conclusions and discussion

Precipitation characteristics, including frequency, intensity, and amount, are often modulated by climate

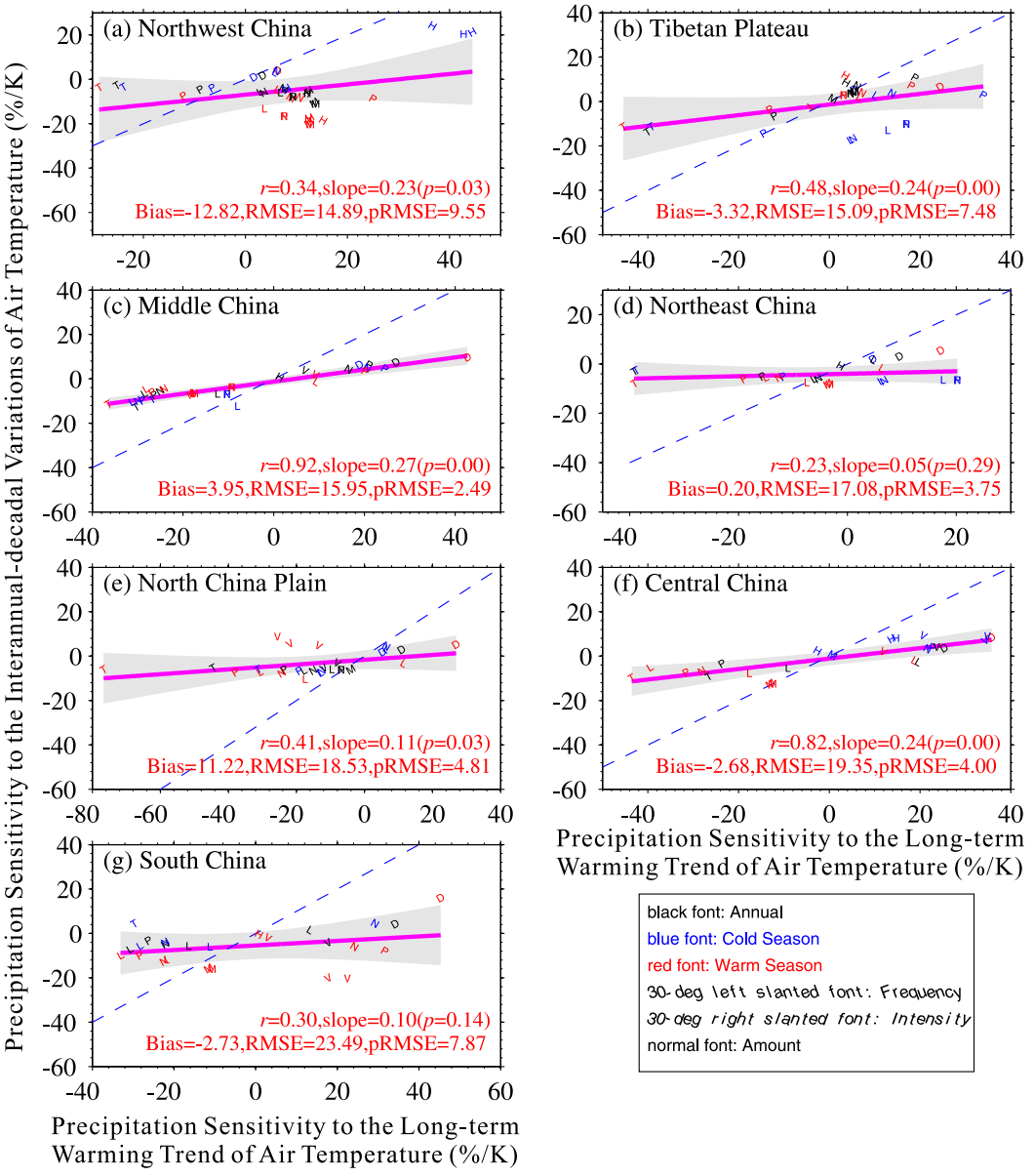

FIG. 12. As in Fig. 11,but for (a) Northwest China, (b) the Tibetan Plateau, (c) Middle China, (d) Northeast China, (e) the North China Plain, (f) Central China, and (g) South China.

changes closely associated with the anthropogenic greenhouse effect and climate variability directly associated with the natural modes of large-scale dynamics. It is generally believed that changes in precipitation are closely linked to global warming, but the magnitude of precipitation sensitivity remains still debated (Trenberth et al. 2003; Zhang et al. 2007; Min et al. 2011; Chou et al. 2012; Marvel and Bonfils 2013). However, precipitation has a huge interannual–decadal variability (e.g., representing over 90% of its total variance in China), which influences the estimate of precipitation sensitivity. In this study, therefore, we disentangled the impacts of climate change and variability on change in precipitation characteristics including precipitation frequency, intensity, and amount over China and its seven subregions.

First, we found that trends in precipitation totals from 1961 to 2014 over China are comparable in both cold and warm seasons, but normalized changes in the cold season are notably larger than those in the warm season, especially in northern China and the Tibetan Plateau. Annual total precipitation has significantly decreased over Middle China and the North China Plain, likely because of a warming trend, human-induced increases in aerosol concentration, and a weakening of the East

Asian monsoons. An increase in precipitation amount over western China and the Tibetan Plateau may result from temperature increases caused by elevated concentrations of anthropogenic greenhouse gases.

Increasing precipitation in southeastern and central China in the cold season has been attributed to weakening of the East Asian winter monsoon (Wang et al. 2009b), enhancement of the Indian monsoon (Wang and Chen 2012), and an abnormal anticyclone over southern Japan, with the northward transport of warm and humid air from the tropical Pacific to southern China (Zhang et al. 2014). Additionally, in Northeast China and Middle China, opposite changes in the precipitation amount have been observed for both seasons.

With long-term temperature increases, the number of dry days increases rapidly with a sensitivity of 14.1% K^{-1} ($p < 0.05$) and that of trace days decreases greatly with a sensitivity of −35.7% K^{-1} ($p < 0.05$) to the warming trend. A decrease in light precipitation frequency by a sensitivity of −14.6% K^{-1} ($p < 0.05$) to the warming trend (−3.1% K^{-1}; $p < 0.05$ to the T_a interannual–decadal variation) leads to a decrease in light precipitation amount by a sensitivity of −4.1% K^{-1} ($p < 0.05$) (−2.6% K^{-1}; $p < 0.05$ to the T_a interannual–decadal variation). Consequently, total precipitation frequency exhibits significant sensitivities to the warming trend (−18.5% K^{-1}; $p < 0.05$) and T_a interannual–decadal variation (−3.6% K^{-1}; $p < 0.05$).

Ma et al. (2015) reported the sensitivities of dry, trace, and light precipitation frequency to change in T_a are 20.63%, −46.53%, and −22.38% K^{-1} ($p < 0.05$), respectively, over China. Our results further reveal that these sensitivities can be divided into two components associated with the long-term trend and interannual–decadal variation of T_a: 14.1%, −35.7%, and −14.6% versus 2.7%, −7.9% and −3.1% K^{-1} ($p < 0.05$). Because of the constraint of available observations, the study period is from 1961 to 2014, which may lead to a result that the long-term trends in precipitation and T_a may contain some multidecadal variation and their interannual–decadal variation may contain some externally forced changes (e.g., decadal aerosol forcing).

A warming trend boosts precipitation intensity to varying extents, being the strongest for light precipitation with an annual sensitivity of 9.8% K^{-1} ($p < 0.05$), while the T_a interannual–decadal variation significantly strongly influence very heavy precipitation intensity (3.7% K^{-1}), especially for the cold season (8% K^{-1}). Consequently, annual total precipitation intensity changes by a sensitivity of 13.1% K^{-1} ($p < 0.05$) to the warming trend and 3.3% K^{-1} ($p < 0.05$) to the T_a interannual–decadal variation. Combining precipitation frequency and intensity, moderate and heavy precipitation amounts are dominated by their frequencies, whereas light and very heavy precipitation amounts are both regulated by their frequencies and intensities. As a result, the annual precipitation amount has a minimal sensitivity to warming trend (0.34% K^{-1}; $p > 0.05$), and the consequent trend of total precipitation in China has a limited trend of 0.08% $decade^{-1}$ ($p > 0.05$). These sensitivities and trends exhibit distinct spatial and seasonal variance in the seven subregions of China because of varying-scale storms, upward motions, moist-convective processes induced by different atmospheric circulations, and convection.

The sensitivities of precipitation in all categories to the interannual–decadal variations are strongly correlated with those to the long-term trend of T_a, with a correlation coefficient of 0.84 ($p = 0.00$), although their magnitudes are not completely consistent. Precipitation sensitivities to the warming trend are approximately 5 times greater than those to the T_a interannual–decadal variation, implying that a human-induced warming trend has an extended and profound impact on precipitation because it is a main contributor to extreme precipitation events.

Acknowledgments. This study was funded by the National Natural Science Foundation of China (41525018 and 91337111) and the National Basic Research Program of China (2012CB955302). The latest precipitation and temperature datasets were obtained from the China Meteorological Administration (CMA; http://data.cma.cn/en).

REFERENCES

Allan, R. P., and B. J. Soden, 2008: Atmospheric warming and the amplification of precipitation extremes. *Science*, **321**, 1481–1484, doi:10.1126/science.1160787.

Allen, M. R., and W. J. Ingram, 2002: Constraints on future changes in climate and the hydrologic cycle. *Nature*, **419**, 224–232, doi:10.1038/nature01092.

Barnston, A. G., and R. E. Livezey, 1987: Classification, seasonality and persistence of low-frequency atmospheric circulation patterns. *Mon. Wea. Rev.*, **115**, 1083–1126, doi:10.1175/1520-0493(1987)115<1083:CSAPOL>2.0.CO;2.

Cheng, Y., U. Lohmann, J. Zhang, Y. Luo, Z. Liu, and G. Lesins, 2005: Contribution of changes in sea surface temperature and aerosol loading to the decreasing precipitation trend in southern China. *J. Climate*, **18**, 1381–1390, doi:10.1175/JCLI3341.1.

Chou, C., and J.-Y. Tu, 2008: Hemispherical asymmetry of tropical precipitation in ECHAM5/MPI-OM during El Niño and under global warming. *J. Climate*, **21**, 1309–1332, doi:10.1175/2007JCLI1928.1.

——, C.-A. Chen, P.-H. Tan, and K. T. Chen, 2012: Mechanisms for global warming impacts on precipitation frequency and intensity. *J. Climate*, **25**, 3291–3306, doi:10.1175/JCLI-D-11-00239.1.

——, J. C. H. Chiang, C. W. Lan, C. H. Chung, Y. C. Liao, and C. J. Lee, 2013: Increase in the range between wet and dry season precipitation. *Nat. Geosci.*, **6**, 263–267, doi:10.1038/ngeo1744.

Conroy, J. L., A. Restrepo, J. T. Overpeck, M. Steinitz-Kannan, J. E. Cole, M. B. Bush, and P. A. Colinvaux, 2009: Unprecedented

recent warming of surface temperatures in the eastern tropical Pacific Ocean. *Nat. Geosci.*, **2**, 46–50, doi:10.1038/ngeo390.

Cubasch, U., and Coauthors, 2001: Projections of future climate change. *Climate Change 2001: The Scientific Basis*, J. T. Houghton et al., Eds., Cambridge University Press, 526–582.

Dai, A., 2001: Global precipitation and thunderstorm frequencies. Part I: Seasonal and interannual variations. *J. Climate*, **14**, 1092–1111, doi:10.1175/1520-0442(2001)014<1092:GPATFP>2.0.CO;2.

——, 2006: Precipitation characteristics in eighteen coupled climate models. *J. Climate*, **19**, 4605–4630, doi:10.1175/JCLI3884.1.

——, 2013: The influence of the inter-decadal Pacific oscillation on US precipitation during 1923–2010. *Climate Dyn.*, **41**, 633–646, doi:10.1007/s00382-012-1446-5.

——, 2016: Future warming patterns linked to today's climate variability. *Sci. Rep.*, **6**, 19110, doi:10.1038/srep19110.

——, and T. Wigley, 2000: Global patterns of ENSO-induced precipitation. *Geophys. Res. Lett.*, **27**, 1283–1286, doi:10.1029/1999GL011140.

Dalton, M. M., and K. M. Shell, 2013: Comparison of short-term and long-term radiative feedbacks and variability in twentieth-century global climate model simulations. *J. Climate*, **26**, 10 051–10 070, doi:10.1175/JCLI-D-12-00564.1.

Deangelis, A. M., X. Qu, M. D. Zelinka, and A. Hall, 2015: An observational radiative constraint on hydrologic cycle intensification. *Nature*, **528**, 249–253, doi:10.1038/nature15770.

Delworth, T. L., and F. Zeng, 2014: Regional rainfall decline in Australia attributed to anthropogenic greenhouse gases and ozone levels. *Nat. Geosci.*, **7**, 583–587, doi:10.1038/ngeo2201.

Denniston, R. F., and Coauthors, 2015: Extreme rainfall activity in the Australian tropics reflects changes in the El Niño/Southern Oscillation over the last two millennia. *Proc. Natl. Acad. Sci. USA*, **112**, 4576–4581, doi:10.1073/pnas.1422270112.

Deser, C., R. Knutti, S. Solomon, and A. S. Phillips, 2012: Communication of the role of natural variability in future North American climate. *Nat. Climate Change*, **2**, 775–779, doi:10.1038/nclimate1562.

Donat, M. G., A. L. Lowry, L. V. Alexander, P. A. Ogorman, and N. Maher, 2016: More extreme precipitation in the world's dry and wet regions. *Nat. Climate Change*, **6**, 508–513, doi:10.1038/nclimate2941.

Dong, B., and A. Dai, 2015: The influence of the interdecadal Pacific oscillation on temperature and precipitation over the globe. *Climate Dyn.*, **45**, 2667–2681, doi:10.1007/s00382-015-2500-x.

Efron, B., and R. J. Tibshirani, 1994: *An Introduction to the Bootstrap*. CRC Press, 456 pp.

Emori, S., and S. Brown, 2005: Dynamic and thermodynamic changes in mean and extreme precipitation under changed climate. *Geophys. Res. Lett.*, **32**, L17706, doi:10.1029/2005GL023272.

Fu, C., and L. Dan, 2014: Trends in the different grades of precipitation over south China during 1960–2010 and the possible link with anthropogenic aerosols. *Adv. Atmos. Sci.*, **31**, 480–491, doi:10.1007/s00376-013-2102-7.

Guillod, B. P., B. Orlowsky, D. G. Miralles, A. J. Teuling, and S. I. Seneviratne, 2015: Reconciling spatial and temporal soil moisture effects on afternoon rainfall. *Nat. Commun.*, **6**, 6443, doi:10.1038/ncomms7443.

Huang, D.-Q., J. Zhu, Y.-C. Zhang, Y. Huang, and X.-Y. Kuang, 2016: Assessment of summer monsoon precipitation derived from five reanalysis datasets over East Asia. *Quart. J. Roy. Meteor. Soc.*, **142**, 108–119, doi:10.1002/qj.2634.

IPCC, 2013: *Climate Change 2013: The Physical Science Basis*. Cambridge University Press, 1535 pp.

——, 2014: *Climate Change 2014: Impacts, Adaptation, and Vulnerability*. Cambridge University Press, 1465 pp. [Available online at Available online at http://www.ipcc.ch/pdf/assessment-report/ar5/wg3/ipcc_wg3_ar5_full.pdf.]

Jiang, Z., Y. Shen, T. Ma, P. Zhai, and S. Fang, 2014: Changes of precipitation intensity spectra in different regions of mainland China during 1961–2006. *J. Meteor. Res.*, **28**, 1085–1098, doi:10.1007/s13351-014-3233-1.

Karl, T. R., and R. W. Knight, 1998: Secular trends of precipitation amount, frequency, and intensity in the United States. *Bull. Amer. Meteor. Soc.*, **79**, 231–241, doi:10.1175/1520-0477(1998)079<0231:STOPAF>2.0.CO;2.

Kharin, V. V., F. W. Zwiers, X. Zhang, and G. C. Hegerl, 2007: Changes in temperature and precipitation extremes in the IPCC ensemble of global coupled model simulations. *J. Climate*, **20**, 1419–1444, doi:10.1175/JCLI4066.1.

Knutti, R., G. A. Meehl, M. R. Allen, and D. A. Stainforth, 2006: Constraining climate sensitivity from the seasonal cycle in surface temperature. *J. Climate*, **19**, 4224–4233, doi:10.1175/JCLI3865.1.

Krzywinski, M., and N. Altman, 2014: Points of significance: Visualizing samples with box plots. *Nat. Methods*, **11**, 119–120, doi:10.1038/nmeth.2813.

Kulesa, A., M. Krzywinski, P. Blainey, and N. Altman, 2015: Points of significance: Sampling distributions and the bootstrap. *Nat. Methods*, **12**, 477–478, doi:10.1038/nmeth.3414.

Lenderink, G., and E. Van Meijgaard, 2008: Increase in hourly precipitation extremes beyond expectations from temperature changes. *Nat. Geosci.*, **1**, 511–514, doi:10.1038/ngeo262.

——, and ——, 2010: Linking increases in hourly precipitation extremes to atmospheric temperature and moisture changes. *Environ. Res. Lett.*, **5**, 025208, doi:10.1088/1748-9326/5/2/025208.

Liu, B., M. Xu, M. Henderson, and Y. Qi, 2005: Observed trends of precipitation amount, frequency, and intensity in China, 1960–2000. *J. Geophys. Res.*, **110**, D08103, doi:10.1029/2004JD004864.

Liu, C. L., and R. P. Allan, 2012: Multisatellite observed responses of precipitation and its extremes to interannual climate variability. *J. Geophys. Res.*, **117**, D03101, doi:10.1029/2011JD016568.

Liu, R., S. C. Liu, R. J. Cicerone, C.-J. Shiu, J. Li, J. Wang, and Y. Zhang, 2015: Trends of extreme precipitation in eastern China and their possible causes. *Adv. Atmos. Sci.*, **32**, 1027–1037, doi:10.1007/s00376-015-5002-1.

Liu, S. C., C. Fu, C.-J. Shiu, J.-P. Chen, and F. Wu, 2009: Temperature dependence of global precipitation extremes. *Geophys. Res. Lett.*, **36**, L17702, doi:10.1029/2009GL040218.

Lu, J., G. Chen, and D. M. Frierson, 2008: Response of the zonal mean atmospheric circulation to El Niño versus global warming. *J. Climate*, **21**, 5835–5851, doi:10.1175/2008JCLI2200.1.

Ma, S., T. Zhou, A. Dai, and Z. Han, 2015: Observed changes in the distributions of daily precipitation frequency and amount over China from 1960 to 2013. *J. Climate*, **28**, 6960–6978, doi:10.1175/JCLI-D-15-0011.1.

Martínez-Casasnovas, J. A., M. C. Ramos, and M. Ribes-Dasi, 2002: Soil erosion caused by extreme rainfall events: Mapping and quantification in agricultural plots from very detailed digital elevation models. *Geoderma*, **105**, 125–140, doi:10.1016/S0016-7061(01)00096-9.

Marvel, K., and C. Bonfils, 2013: Identifying external influences on global precipitation. *Proc. Natl. Acad. Sci. USA*, **110**, 19 301–19 306, doi:10.1073/pnas.1314382110.

Menon, S., J. Hansen, L. Nazarenko, and Y. Luo, 2002: Climate effects of black carbon aerosols in China and India. *Science*, **297**, 2250–2253, doi:10.1126/science.1075159.

Min, S. K., X. Zhang, F. W. Zwiers, and G. C. Hegerl, 2011: Human contribution to more-intense precipitation extremes. *Nature*, **470**, 378–381, doi:10.1038/nature09763.

Mishra, A., and S. C. Liu, 2014: Changes in precipitation pattern and risk of drought over India in the context of global warming. *J. Geophys. Res. Atmos.*, **119**, 7833–7841, doi:10.1002/2014JD021471.

Mooley, D. A., 1973: Gamma distribution probability model for Asian summer monsoon monthly rainfall. *Mon. Wea. Rev.*, **101**, 160–176, doi:10.1175/1520-0493(1973)101<0160:GDPMFA>2.3.CO;2.

O'Gorman, P. A., 2012: Sensitivity of tropical precipitation extremes to climate change. *Nat. Geosci.*, **5**, 697–700, doi:10.1038/ngeo1568.

——, and T. Schneider, 2009a: Scaling of precipitation extremes over a wide range of climates simulated with an idealized GCM. *J. Climate*, **22**, 5676–5685, doi:10.1175/2009JCLI2701.1.

——, and ——, 2009b: The physical basis for increases in precipitation extremes in simulations of 21st-century climate change. *Proc. Natl. Acad. Sci. USA*, **106**, 14 773–14 777, doi:10.1073/pnas.0907610106.

Podobnik, B., and H. E. Stanley, 2008: Detrended cross-correlation analysis: A new method for analyzing two nonstationary time series. *Phys. Rev. Lett.*, **100**, 084102, doi:10.1103/PhysRevLett.100.084102.

Qian, Y., D. Gong, J. Fan, L. R. Leung, R. Bennartz, D. Chen, and W. Wang, 2009: Heavy pollution suppresses light rain in China: Observations and modeling. *J. Geophys. Res.*, **114**, D00K02, doi:10.1029/2008JD011575.

Shiu, C.-J., S. C. Liu, C. Fu, A. Dai, and Y. Sun, 2012: How much do precipitation extremes change in a warming climate? *Geophys. Res. Lett.*, **39**, L17707, doi:10.1029/2012GL052762.

Siswanto, G. J. van Oldenborgh, G. van der Schrier, G. Lenderink, and B. van den Hurk, 2015: Trends in high-daily precipitation events in Jakarta and the flooding of January 2014 [in "Explaining Extreme Events of 2014"]. *Bull. Amer. Meteor. Soc.*, **96** (12), S131–S135, doi:10.1175/BAMS-D-15-00128.1.

Smith, T. M., X. Yin, and A. Gruber, 2006: Variations in annual global precipitation (1979–2004), based on the Global Precipitation Climatology Project 2.5° analysis. *Geophys. Res. Lett.*, **33**, L06705, doi:10.1029/2005GL025393.

Stephens, G. L., and T. D. Ellis, 2008: Controls of global-mean precipitation increases in global warming GCM experiments. *J. Climate*, **21**, 6141–6155, doi:10.1175/2008JCLI2144.1.

Sun, Y., S. Solomon, A. Dai, and R. W. Portmann, 2007: How often will it rain? *J. Climate*, **20**, 4801–4818, doi:10.1175/JCLI4263.1.

Trenberth, K. E., 1998: Atmospheric moisture residence times and cycling: Implications for rainfall rates and climate change. *Climatic Change*, **39**, 667–694, doi:10.1023/A:1005319109110.

——, and D. J. Shea, 2005: Relationships between precipitation and surface temperature. *Geophys. Res. Lett.*, **32**, L14703, doi:10.1029/2005GL022760.

——, G. W. Branstator, D. Karoly, A. Kumar, N. C. Lau, and C. Ropelewski, 1998: Progress during TOGA in understanding and modeling global teleconnections associated with tropical sea surface temperatures. *J. Geophys. Res.*, **103**, 14 291–14 324, doi:10.1029/97JC01444.

——, A. Dai, R. M. Rasmussen, and D. B. Parsons, 2003: The changing character of precipitation. *Bull. Amer. Meteor. Soc.*, **84**, 1205–1217, doi:10.1175/BAMS-84-9-1205.

Veizer, J., Y. Godderis, and L. M. Francois, 2000: Evidence for decoupling of atmospheric CO_2 and global climate during the Phanerozoic eon. *Nature*, **408**, 698–701, doi:10.1038/35047044.

Wang, H., 2001: The weakening of the Asian monsoon circulation after the end of 1970's. *Adv. Atmos. Sci.*, **18**, 376–386, doi:10.1007/BF02919316.

——, and H. P. Chen, 2012: Climate control for southeastern China moisture and precipitation: Indian or East Asian monsoon? *J. Geophys. Res.*, **117**, D12109, doi:10.1029/2012JD017734.

Wang, L., W. Chen, W. Zhou, and R. Huang, 2009a: Interannual variations of East Asian trough axis at 500 hPa and its association with the East Asian winter monsoon pathway. *J. Climate*, **22**, 600–614, doi:10.1175/2008JCLI2295.1.

——, R. Huang, L. Gu, W. Chen, and L. Kang, 2009b: Interdecadal variations of the East Asian winter monsoon and their association with quasi-stationary planetary wave activity. *J. Climate*, **22**, 4860–4872, doi:10.1175/2009JCLI2973.1.

Wang, Y., and L. Zhou, 2005: Observed trends in extreme precipitation events in China during 1961–2001 and the associated changes in large-scale circulation. *Geophys. Res. Lett.*, **32**, L09707, doi:10.1029/2005GL023769.

——, P. L. Ma, J. H. Jiang, H. Su, and P. J. Rasch, 2016: Toward reconciling the influence of atmospheric aerosols and greenhouse gases on light precipitation changes in eastern China. *J. Geophys. Res. Atmos.*, **121**, 5878–5887, doi:10.1002/2016JD024845.

Wasko, C., and A. Sharma, 2015: Steeper temporal distribution of rain intensity at higher temperatures within Australian storms. *Nat. Geosci.*, **8**, 527–529, doi:10.1038/ngeo2456.

Westra, S., L. V. Alexander, and F. W. Zwiers, 2013: Global increasing trends in annual maximum daily precipitation. *J. Climate*, **26**, 3904–3918, doi:10.1175/JCLI-D-12-00502.1.

——, and Coauthors, 2014: Future changes to the intensity and frequency of short-duration extreme rainfall. *Rev. Geophys.*, **52**, 522–555, doi:10.1002/2014RG000464.

Wu, R., J. Chen, and Z. Wen, 2013: Precipitation-surface temperature relationship in the IPCC CMIP5 models. *Adv. Atmos. Sci.*, **30**, 766–778, doi:10.1007/s00376-012-2130-8.

Xu, Q., 2001: Abrupt change of the mid-summer climate in central east China by the influence of atmospheric pollution. *Atmos. Environ.*, **35**, 5029–5040, doi:10.1016/S1352-2310(01)00315-6.

Zhai, P., X. Zhang, H. Wan, and X. Pan, 2005: Trends in total precipitation and frequency of daily precipitation extremes over China. *J. Climate*, **18**, 1096–1108, doi:10.1175/JCLI-3318.1.

Zhang, L., X. H. Zhu, K. Fraedrich, F. Sielmann, and X. F. Zhi, 2014: Interdecadal variability of winter precipitation in southeast China. *Climate Dyn.*, **43**, 2239–2248, doi:10.1007/s00382-014-2048-1.

Zhang, X., and Coauthors, 2007: Detection of human influence on twentieth-century precipitation trends. *Nature*, **448**, 461–465, doi:10.1038/nature06025.

Zhao, C. S., X. X. Tie, and Y. P. Lin, 2006: A possible positive feedback of reduction of precipitation and increase in aerosols over eastern central China. *Geophys. Res. Lett.*, **33**, L11816, doi:10.1029/2006GL025959.

Zhou, L., R. E. Dickinson, Y. Tian, R. S. Vose, and Y. Dai, 2007: Impact of vegetation removal and soil aridation on diurnal temperature range in a semiarid region: Application to the Sahel. *Proc. Natl. Acad. Sci. USA*, **104**, 17 937–17 942, doi:10.1073/pnas.0700290104.

Zhou, L.-T., and R.-H. Huang, 2010: Interdecadal variability of summer rainfall in northwest China and its possible causes. *Int. J. Climatol.*, **30**, 549–557, doi:10.1002/joc.1923.